

---

# Self-Attentive Ensemble Transformer: Representing Ensemble Interactions in Neural Networks for Earth System Models

---

Tobias Sebastian Finn<sup>1 2</sup>

## Abstract

Ensemble data from Earth system models has to be calibrated and post-processed. I propose a novel member-by-member post-processing approach with neural networks. I bridge ideas from ensemble data assimilation with self-attention, resulting into the self-attentive ensemble transformer. Here, interactions between ensemble members are represented as additive and dynamic self-attentive part. As proof-of-concept, global ECMWF ensemble forecasts are regressed to 2-metre-temperature fields from the ERA5 reanalysis. I demonstrate that the ensemble transformer can calibrate the ensemble spread and extract additional information from the ensemble. Furthermore, the ensemble transformer directly outputs multivariate and spatially-coherent ensemble members. Therefore, self-attention and the transformer technique can be a missing piece for a member-by-member post-processing of ensemble data with neural networks.

## 1. Introduction

In Earth system modelling, an ensemble of simulations (Leith, 1974) is a Monte-Carlo approach to estimate the uncertainties within weather predictions (Bauer et al., 2015; Molteni et al., 1996; Toth & Kalnay, 1993) or to assess the internal variability within the Earth system (Deser et al., 2020; Kay et al., 2015; Maher et al., 2019). Every ensemble member is physically-consistent in their multivariate structure. The ensemble can thus represent non-linear evolutions and non-Gaussian distributed states as they appear in nature. Nevertheless, ensembles have to be post-processed (Hemri et al., 2014; Steining et al., 2020) by model output statis-

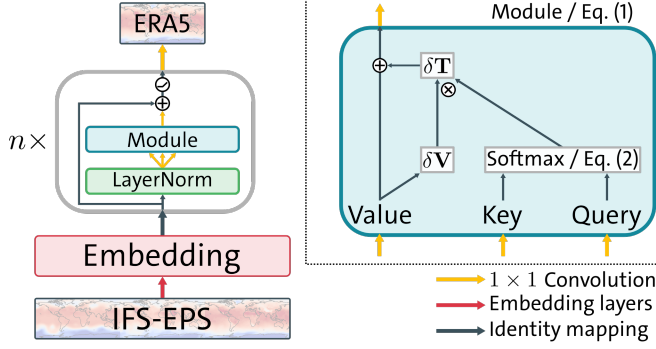
tics to correct model biases and predict unmodelled variables. Often, summarized ensemble statistics are targeted by post-processing (Schulz & Lerch, 2021), predicting either the parameters (Gneiting et al., 2005; Raftery et al., 2005; Rasp & Lerch, 2018) or the cumulative distribution function (Baran & Lerch, 2018; Bremnes, 2020; Scheuerer et al., 2020; Taillardat et al., 2016) of the target distribution. As a consequence, the member-wise multivariate and spatial-coherent representation of the ensemble forecast is lost. By contrast, I propose a member-by-member post-processing approach (Schaeysbroeck & Vannitsem, 2015) with neural networks and a self-attentive ensemble transformer.

If neural networks are independently applied on each member, the ensemble members are not informed about the evolution of other ensemble members. This results into a loss of information and to problems of calibrating the ensemble spread. In a linear update step, ensemble Kalman filters (Bishop et al., 2001; Burgers et al., 1998; Evensen, 1994) solve this problem by using predicted ensemble covariances to assimilate given observations into ensemble predictions. In this way, they include interactions between ensemble members.

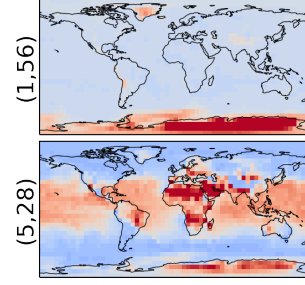
In their core approach, ensemble Kalman filters are similar to (self-)attention modules (Luong et al., 2015; Vaswani et al., 2017; Wang et al., 2018) for neural networks, despite having another terminology: the value in attention modules or the state in ensemble Kalman filters is modified based on weights, estimated with keys (the adjoint in ensemble Kalman filters) and queries (observations). In the so-called self-attention modules, the keys and queries are projections of the same embedding that is also used to project the values. The module literally informs itself about the searched information.

By bridging ideas of ensemble Kalman filtering with self-attention, I introduce the self-attentive ensemble transformer as neural network for processing of ensemble data. Estimated with self-attention, each module adds to the static value of each ensemble member a dynamic self-attentive part that represents the interactions between ensemble members. It thus can be seen as set transformer (Lee et al., 2019). By regressing ECMWF ensemble forecasts to ERA5 reanalyses, I demonstrate that ensemble transformers can calibrate

<sup>1</sup>Meteorological Institute, University of Hamburg, Hamburg, Germany <sup>2</sup>International Max Planck Research School on Earth System Modelling, Max Planck Institute for Meteorology, Hamburg, Germany. Correspondence to: Tobias Sebastian Finn <tobias.sebastian.finn@uni-hamburg.de>.



(a) Schematic overview of the ensemble transformer architecture. The separated side of the figure is a zoom-in to a single module.



(b) Two selected attention maps (layer number, head number) from the Transformer (5) experiment for 2019-09-01 12:00 UTC. The shown maps represent possibly regions with temperatures below the freezing level and with precipitation anomalies.

Figure 1. Schematic overview of the self-attentive ensemble transformer module and exemplary attention maps.

the ensemble and correct model errors. In addition, the transformer outputs multivariate and spatially-coherent ensemble members. This proves that current developments in machine learning can be also used to improve post-processing of Earth system modelling.

## 2. The self-attentive ensemble transformer

In the following, I introduce a self-attentive transformer module as single neural network layer. A schematic overview over the architecture and module can be found in Figure 1a.

Let  $\mathbf{Z}_l \in \mathbb{R}^{k \times c \times h \times w}$  be the input to the  $l$ -th layer with  $k$  as ensemble members,  $c$  as channels,  $h$  as height, and  $w$  as width. The goal of the module is to estimate the transformed output  $\mathbf{t}_i(\mathbf{Z}_l) \in \mathbb{R}^{c \times h \times w}$  of the  $i$ -th member based on the input of all members. This transformed output is split into a static part  $\mathbf{v}_i$  and a dynamic part  $\delta \mathbf{t}_i(\mathbf{Z}_l)$ . The static part, also called value, is a linear projection of the input  $\mathbf{V} = \mathbf{Z}_l \mathbf{W}_l^v$  with  $\mathbf{W}_l^v \in \mathbb{R}^{c \times \tilde{c}}$  as linear projection matrix and  $\tilde{c}$  as the number of heads. The dynamic part adds information from all members to the current  $i$ -th member, as it is similarly done in ensemble data assimilation (Bishop et al., 2001; Hunt et al., 2007; Lorenc, 2003). I represent this dynamic part as additive and linear combination of the value perturbations by ensemble weights  $\mathbf{w}_i \in \mathbb{R}^{\tilde{c} \times k}$  with  $\bar{\mathbf{v}} = k^{-1} \sum_{j=1}^k \mathbf{v}_j$  as the ensemble mean of the values and  $\delta \mathbf{V}$  as collected perturbations of all members,

$$\mathbf{t}_i(\mathbf{Z}_l) = \mathbf{v}_i + \delta \mathbf{t}_i(\mathbf{Z}_l) = \mathbf{v}_i + \sum_{j=1}^k (\mathbf{v}_j - \bar{\mathbf{v}}) \mathbf{w}_{i,j}. \quad (1)$$

In ensemble Kalman filters, the weights are estimated based on the similarity between given observations and the ensemble members projected into observational space. For post-processing and prediction purpose, no observations are available. The transformer module has thus to rely on

self-attention. In self-attention, the weights are estimated based on the same input data as the values (Vaswani et al., 2017; Wang et al., 2018). Here, the observations are replaced by a query  $\mathbf{q}_i \in \mathbb{R}^{\tilde{c} \times h \times w}$ , representing the searched information for the current  $i$ -th member. This query has to be related to the value perturbations of all members to estimate the weights. Such a relation is represented by a key matrix  $\mathbf{K} \in \mathbb{R}^{k \times \tilde{c} \times h \times w}$ , replacing the adjoint in data assimilation. Both, the query and the key matrix are again linear projections of the input data with  $\mathbf{W}_l^q \in \mathbb{R}^{c \times \tilde{c}}$  and  $\mathbf{W}_l^k \in \mathbb{R}^{c \times \tilde{c}}$  as projection matrices.

Similar to Vaswani et al. (2017), the similarity is cast as scaled dot product between the query and key matrix  $\mathbf{K}(\mathbf{q}_i)^T \in \mathbb{R}^{\tilde{c} \times k}$  over the height and weight. To obtain non-negative weights for a convex combination of value perturbations, the scaled-dot product is squashed through a softmax activation, leading to

$$\mathbf{w}_i = \frac{\tilde{\mathbf{w}}_i}{\sum_{j=1}^k \tilde{\mathbf{w}}_{i,j}}, \quad \tilde{\mathbf{w}}_i = \exp\left(\frac{\mathbf{K}(\mathbf{q}_i)^T}{\sqrt{h \times w}}\right). \quad (2)$$

With these weights, I explicitly make use of the permutation-invariance in self-attention for ensemble data.

The output of the transformer module is modelled as residual connection (He et al., 2015) with  $\mathbf{T}(\mathbf{Z}_l) \in \mathbb{R}^{k \times \tilde{c} \times h \times w}$  as the collection of all transformed members from (1). The residual branch is linearly projected by  $\mathbf{W}_l^o \in \mathbb{R}^{\tilde{c} \times c}$  from the attentive space back into the original feature space of the identity mapping. I initialize  $\mathbf{W}_l^o$  as all-zero matrix; thus, only the identity mapping is used at the beginning of the training. I activate the output of the residual layer with an activation function  $f_i$ , here the rectified linear unit (ReLU). This results into the input  $\mathbf{Z}_{l+1}$  of the next layer,

$$\mathbf{Z}_{l+1} = f_i(\mathbf{Z}_l + \mathbf{W}_l^o \mathbf{T}(\mathbf{Z}_l)). \quad (3)$$

This finishes the description of a single transformer module.

Since  $\delta t_i(\mathbf{Z}_i)$  is a convex combination of value perturbations, one single-layered ensemble transformer module might be not expressive enough. To extract more complex and non-linear interactions between ensemble members, it might be thus advantageous to stack multiple modules onto each other.

The ensemble space ( $k = 50$ ) is normally much smaller than the spatial space (in my case  $h \times w = 2048$ ). Because the weights are estimated in this ensemble space, spatially-global self-attention can be performed efficiently by (1) and (2). The weights for all ensemble members can be then estimated in parallel with  $\mathbf{Q} \in \mathbb{R}^{k \times \tilde{c} \times h \times w}$  as the collection of all queries for all members. The costs of the ensemble transformer scales quadratically with the number of members, but the weight formulation allows training with another number of members than used for inference, as I show later.

As the dot product is estimated over spatial dimensions, the channels  $\tilde{c}$  within the attentive space are similar to multiple heads in standard self-attention. The channels can thus represent different attentive regions. To discover such regions with high influence, the element-wise product  $\bar{\mathbf{k}} \cdot \bar{\mathbf{q}} \in \mathbb{R}^{\tilde{c} \times h \times w}$  of the ensemble mean key  $\bar{\mathbf{k}} = k^{-1} \sum_{j=1}^k \mathbf{k}_j$  and the ensemble mean query  $\bar{\mathbf{q}} = k^{-1} \sum_{j=1}^k \mathbf{q}_j$  can be used, as exemplary shown in Figure 1b.

### 3. Experiments and Discussion

In a first step, I explain the used architectures and training methods. As second step, I discuss and visualize the results from these experiments.

#### 3.1. Experimental strategy

As input, I use data from the ECMWF ensemble prediction system (IFS-EPS, ECMWF (2019)) with  $k = 50$  ensemble members and three variables: the geopotential height on the 500 hPa pressure level, the temperature on the 850 hPa pressure level, and the 2-metre-temperature. The forecasts with a lead time of 48 hours are valid for 00:00Z and 12:00Z. They are fitted to the 2-metre-temperature of the ERA5 reanalysis project (Hersbach et al., 2020). The whole dataset consists of three-years data (2017-2019): 2017 and 2018 are used for training and validation, whereas 2019 is used for testing purpose. I randomly select 10% of 2017 and 2018 for validation. As pre-processing, the global fields are bilinearly regridded to  $h \times w = 32 \times 64$  grid points, as in Rasp et al. (2020). The input data is normalized by their global mean and standard deviation, fitted for every variable independently based on the training dataset.

For all of my experiments, I use the same initial embedding structure with three consecutive two-dimensional convolutional layers, which are applied on every ensemble member

independently. For these convolutions, I use a kernel size of  $5 \times 5$  with a locally-equidistant assumption,  $c = 64$  channels, and the ReLU activation. I circularly pad in longitudinal direction and zero-pad in latitudinal direction.

In the **Transformer** experiments, I stack  $n$  ensemble transformer modules between the embedding and the output. For linear projections within the transformer layers, I use  $1 \times 1$  convolutions with  $\tilde{c} = 64$  heads. As proposed in (Xiong et al., 2020), I apply layer normalization (Ba et al., 2016) across the channels, latitudes, and longitudes before linearly projecting the module input. As output layer, I use a  $1 \times 1$  convolution, combining information from 64 channels into the 2-metre-temperature for each member independently.

As baseline, I post-process each member independently without any transformer module in the **Direct** experiments. In addition, I apply a parametric neural network (PPNN, Rasp & Lerch (2018)). Here, the output of the embedding is averaged over the members and concatenated with the ensemble mean and standard deviation of the inputted 2-metre-temperature, as in Rasp & Lerch (2018). In the **PPNN** experiments, the output is parametrized as the ensemble mean and standard deviation.

In these baseline experiments, I use  $n$  additional residual layers (He et al., 2015) between embedding and output. These layers are two  $1 \times 1$  convolutions with 64 channels and the ReLU activation function in-between. I have modified and initialized these residual layers in correspondence to (Zhang et al., 2019). They are thus similar to the residual layer within the transformer module without self-attention.

As loss function, I minimize for all experiments the continuously ranked probability score (CRPS, Gneiting & Raftery (2007); Hersbach (2000)) with a Gaussian assumption and latitudinal weighting as in Rasp et al. (2020). For the transformer and direct experiments, I calculate the ensemble mean and the bessel-corrected ensemble standard deviation from the resulting ensemble members as CRPS estimation step. I have trained all models on a Nvidia GeForce GTX 1060 with a batch size of 8 samples. Each experiment is optimized with Adam (Kingma & Ba, 2017) and an initial learning rate of  $1 \times 10^{-3}$ . If the validation CRPS is not decreasing for 5 epochs, the learning rate is multiplied with 0.3 of its previous value. The training is ended if the validation CRPS is not decreasing for 20 epochs or after 200 epochs. I implemented<sup>1</sup> the models with PyTorch (Paszke et al., 2019).

#### 3.2. Results

To compare the experiments (Table 1 and Table 2), I evaluate the latitudinal weighted spatio-temporal mean CRPS

<sup>1</sup>Implementation can be found under: [https://github.com/tobifinn/ensemble\\_transformer](https://github.com/tobifinn/ensemble_transformer)

Table 1. The CRPS to the reanalysis, the ensemble mean RMSE, and the mean ensemble spread in the test dataset for all 50 ensemble members. The number behind the experiments indicates how many members were subsampled in each training sample.

Name (members)	CRPS	RMSE (K)	Spread (K)
Transformer (10)	0.42	0.91	0.91
Transformer (20)	0.42	0.92	0.90
Transformer (50)	0.42	0.92	0.89

to the ERA5 reanalysis, the weighted spatio-temporal root-mean-squared-error of the ensemble mean (RMSE), and the square-root of the latitudinal weighted spatio-temporal mean of the ensemble variance (Spread).

The training speed depends on the number of ensemble members that are used during the training. To reduce the trainings costs, the ensemble can be subsampled by randomly selecting fewer members for each training sample (Table 1). Because of additional noise, smaller subsampled sizes help to regularize the networks, but a too small subsampled ensemble might lead to an unstable training. To strike a balance, I subsample 20 members in each training sample for all subsequent experiments.

Table 2. The CRPS, the ensemble mean RMSE, and the ensemble standard deviation in the test dataset. The number behind the experiments indicates how many additional layers between embedding and output layer are used.

Name (layers)	CRPS	RMSE (K)	Spread (K)
Climatology	2.60	6.12	6.05
IFS-EPS raw	0.52	1.12	0.73
PPNN (0)	0.44	0.96	0.87
PPNN (1)	0.43	0.95	0.87
PPNN (5)	0.42	0.93	0.87
Direct (1)	0.45	0.95	0.70
Direct (5)	0.45	0.96	0.70
Transformer (1)	0.42	0.91	0.91
Transformer (5)	0.41	0.90	0.90

The general performance of all methods is bounded by the available information from the input fields, as can be seen in Table 2. Nevertheless, the RMSE and CRPS of the PPNN and transformer networks scale slightly with increasing network depth. In addition, the predictions of the PPNN and Transformer are calibrated (a PIT histogram is shown in Appendix A), whereas the direct approach without self-attention has problems to match the ensemble spread to the RMSE. Therefore, the self-attention mechanism is not only able to spread the ensemble members out, but also to extract additional information from the interactions between ensemble members. As a result, the ensemble transformer is the best performing method in these experiments even compared to the parametric PPNN approach.

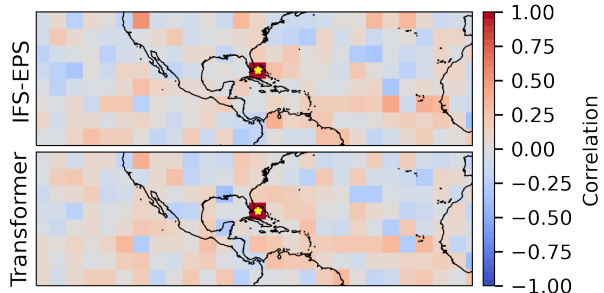


Figure 2. The spatial correlation within the 50 ensemble members from the IFS-EPS data and the Transformer(5) experiment at 01th September 2019, 12:00 UTC, estimated to the yellow-marked grid point of interest, the position of Hurricane Dorian.

Linear spatial patterns within the ensemble members can be found by analysing the ensemble correlation structure (Figure 2). Here, the post-processed ensemble members represent similar correlation structures as they can be found within the raw IFS-EPS ensemble. Normally, additional methods like Gaussian copulas (Lerch et al., 2020; Schefzik et al., 2013) are needed to represent such multivariate structures within a post-processed ensemble. The ensemble transformer is a member-by-member approach and adds interactions between ensemble members as dynamic term. It can thus directly output spatially-coherent ensemble members, despite only targeting an univariately spatio-temporal averaged CRPS during training.

## 4. Conclusion

Based on the results of post-processing global ECMWF ensemble predictions to ERA5 2-metre-temperature reanalyses with ensemble transformers and convolutional neural networks, I conclude the following:

- Self-attention can inform ensemble members about the evolution of other members within a neural network. Global self-attention can be hereby efficiently represented within the space of the ensemble members.
- The ensemble transformer can calibrate the ensemble spread. Furthermore, it can extract additional information from the interactions between ensemble members.
- Ensemble transformer can directly process ensemble members without using ensemble statistics and output again multivariate and spatially-coherent ensemble members.

Therefore, the self-attentive ensemble transformer can be a missing piece for a member-by-member post-processing of ensemble data with neural networks and without using summarized ensemble statistics.

## 5. Acknowledgements

This work is a contribution to the research unit FOR2131, "Data Assimilation for Improved Characterization of Fluxes across Compartmental Interfaces", funded by the "Deutsche Forschungsgemeinschaft" (DFG, German Research Foundation) under grant 243358811. I would like to acknowledge the ECMWF for providing the IFS-EPS data via the "The International Grand Global Ensemble" project and the Copernicus Climate Change Service (C3S) for distributing the ERA5 reanalysis data (Hersbach et al., 2020), downloaded from the Climate Data Store.

## References

- Ba, J. L., Kiros, J. R., and Hinton, G. E. Layer Normalization. *ArXiv160706450 Cs Stat*, July 2016.
- Baran, S. and Lerch, S. Combining predictive distributions for the statistical post-processing of ensemble forecasts. *International Journal of Forecasting*, 34(3):477–496, July 2018. ISSN 0169-2070. doi: 10.1016/j.ijforecast.2018.01.005.
- Bauer, P., Thorpe, A., and Brunet, G. The quiet revolution of numerical weather prediction. *Nature*, 525(7567):47–55, 2015. ISSN 1476-4687. doi: 10.1038/nature14956.
- Bishop, C. H., Etherton, B. J., and Majumdar, S. J. Adaptive Sampling with the Ensemble Transform Kalman Filter. Part I: Theoretical Aspects. *Mon. Wea. Rev.*, 129(3):420–436, March 2001. ISSN 0027-0644. doi: 10.1175/1520-0493(2001)129<0420:ASWTET>2.0.CO;2.
- Bremnes, J. B. Ensemble Postprocessing Using Quantile Function Regression Based on Neural Networks and Bernstein Polynomials. *Mon. Weather Rev.*, 148(1):403–414, January 2020. ISSN 1520-0493, 0027-0644. doi: 10.1175/MWR-D-19-0227.1.
- Burgers, G., Jan van Leeuwen, P., and Evensen, G. Analysis Scheme in the Ensemble Kalman Filter. *Mon. Wea. Rev.*, 126(6):1719–1724, June 1998. ISSN 0027-0644. doi: 10.1175/1520-0493(1998)126<1719:ASITEK>2.0.CO;2.
- Deser, C., Lehner, F., Rodgers, K. B., Ault, T., Delworth, T. L., DiNezio, P. N., Fiore, A., Frankignoul, C., Fyfe, J. C., Horton, D. E., Kay, J. E., Knutti, R., Lovenduski, N. S., Marotzke, J., McKinnon, K. A., Minobe, S., Randerson, J., Screen, J. A., Simpson, I. R., and Ting, M. Insights from Earth system model initial-condition large ensembles and future prospects. *Nat. Clim. Change*, 10(4):277–286, April 2020. ISSN 1758-6798. doi: 10.1038/s41558-020-0731-2.
- ECMWF. *IFS Documentation CY46R1*. IFS Documentation. 2019.
- Evensen, G. Sequential data assimilation with a nonlinear quasi-geostrophic model using Monte Carlo methods to forecast error statistics. *J. Geophys. Res. Oceans*, 99(C5):10143–10162, 1994. ISSN 2156-2202. doi: 10.1029/94JC00572.
- Gneiting, T. and Raftery, A. E. Strictly Proper Scoring Rules, Prediction, and Estimation. *Journal of the American Statistical Association*, 102(477):359–378, March 2007. ISSN 0162-1459, 1537-274X. doi: 10.1198/016214506000001437.
- Gneiting, T., Raftery, A. E., Westveld, A. H., and Goldman, T. Calibrated Probabilistic Forecasting Using Ensemble Model Output Statistics and Minimum CRPS Estimation. *Mon. Weather Rev.*, 133(5):1098–1118, May 2005. ISSN 1520-0493, 0027-0644. doi: 10.1175/MWR2904.1.
- He, K., Zhang, X., Ren, S., and Sun, J. Deep Residual Learning for Image Recognition. *ArXiv151203385 Cs*, December 2015.
- Hemri, S., Scheuerer, M., Pappenberger, F., Bogner, K., and Haiden, T. Trends in the predictive performance of raw ensemble weather forecasts. *Geophys. Res. Lett.*, 41(24):9197–9205, 2014. ISSN 1944-8007. doi: 10.1002/2014GL062472.
- Hersbach, H. Decomposition of the Continuous Ranked Probability Score for Ensemble Prediction Systems. *WEATHER Forecast.*, 15:12, 2000.
- Hersbach, H., Bell, B., Berrisford, P., Hirahara, S., Horányi, A., Muñoz-Sabater, J., Nicolas, J., Peubey, C., Radu, R., Schepers, D., Simmons, A., Soci, C., Abdalla, S., Abellan, X., Balsamo, G., Bechtold, P., Biavati, G., Bidlot, J., Bonavita, M., Chiara, G. D., Dahlgren, P., Dee, D., Diamantakis, M., Dragani, R., Flemming, J., Forbes, R., Fuentes, M., Geer, A., Haimberger, L., Healy, S., Hogan, R. J., Hólm, E., Janisková, M., Keeley, S., Laloyaux, P., Lopez, P., Lupu, C., Radnoti, G., de Rosnay, P., Rozum, I., Vamborg, F., Villaume, S., and Thépaut, J.-N. The ERA5 global reanalysis. *Q. J. R. Meteorol. Soc.*, 146(730):1999–2049, 2020. ISSN 1477-870X. doi: 10.1002/qj.3803.
- Hunt, B. R., Kostelich, E. J., and Szunyogh, I. Efficient data assimilation for spatiotemporal chaos: A local ensemble transform Kalman filter. *Physica D: Nonlinear Phenomena*, 230(1):112–126, June 2007. ISSN 0167-2789. doi: 10.1016/j.physd.2006.11.008.
- Kay, J. E., Deser, C., Phillips, A., Mai, A., Hannay, C., Strand, G., Arblaster, J. M., Bates, S. C., Danabasoglu, G., Edwards, J., Holland, M., Kushner, P., Lamarque, J.-F., Lawrence, D., Lindsay, K., Middleton, A., Muñoz, E., Neale, R., Oleson, K., Polvani, L., and Vertenstein, M. The Community Earth System Model (CESM) Large Ensemble Project: A Community Resource for Studying Climate Change in the Presence of Internal Climate Variability. *Bull. Am. Meteorol. Soc.*, 96(8):1333–1349, August 2015. ISSN 0003-0007, 1520-0477. doi: 10.1175/BAMS-D-13-00255.1.
- Kingma, D. P. and Ba, J. Adam: A Method for Stochastic Optimization. *ArXiv14126980 Cs*, January 2017.
- Lee, J., Lee, Y., Kim, J., Kosiorek, A. R., Choi, S., and Teh, Y. W. Set Transformer: A Framework for Attention-based Permutation-Invariant Neural Networks. *ArXiv181000825 Cs Stat*, May 2019.
- Leith, C. E. Theoretical Skill of Monte Carlo Forecasts. *Mon. Weather Rev.*, 102(6):409–418, June 1974. ISSN 1520-0493, 0027-0644. doi: 10.1175/1520-0493(1974)102<0409:TSOMCF>2.0.CO;2.
- Lerch, S., Baran, S., Möller, A., Groß, J., Schefzik, R., Hemri, S., and Graeter, M. Simulation-based comparison of multivariate ensemble post-processing methods. *Nonlinear Process. Geophys.*, 27(2):349–371, June 2020. ISSN 1023-5809. doi: 10.5194/npg-27-349-2020.

- Lorenc, A. C. The potential of the ensemble Kalman filter for NWP—a comparison with 4D-Var. *Q. J. R. Meteorol. Soc.*, 129 (595):3183–3203, 2003. ISSN 1477-870X. doi: 10.1256/qj.02.132.
- Luong, M.-T., Pham, H., and Manning, C. D. Effective Approaches to Attention-based Neural Machine Translation. *ArXiv150804025 Cs*, September 2015.
- Maher, N., Milinski, S., Suarez-Gutierrez, L., Botzet, M., Dobrynin, M., Kornbluh, L., Kröger, J., Takano, Y., Ghosh, R., Hedemann, C., Li, C., Li, H., Manzini, E., Notz, D., Putrasahan, D., Boysen, L., Claussen, M., Ilyina, T., Olonscheck, D., Radatz, T., Stevens, B., and Marotzke, J. The Max Planck Institute Grand Ensemble: Enabling the Exploration of Climate System Variability. *J. Adv. Model. Earth Syst.*, 11(7):2050–2069, 2019. ISSN 1942-2466. doi: 10.1029/2019MS001639.
- Molteni, F., Buizza, R., Palmer, T. N., and Petroliagis, T. The ECMWF Ensemble Prediction System: Methodology and validation. *Q. J. R. Meteorol. Soc.*, 122(529):73–119, 1996. ISSN 1477-870X. doi: 10.1002/qj.49712252905.
- Paszke, A., Gross, S., Massa, F., Lerer, A., Bradbury, J., Chanan, G., Killeen, T., Lin, Z., Gimelshein, N., Antiga, L., Desmaison, A., Kopf, A., Yang, E., DeVito, Z., Raison, M., Tejani, A., Chilamkurthy, S., Steiner, B., Fang, L., Bai, J., and Chintala, S. PyTorch: An Imperative Style, High-Performance Deep Learning Library. In Wallach, H., Laroche, H., Beygelzimer, A., Alché-Buc, F., Fox, E., and Garnett, R. (eds.), *Advances in Neural Information Processing Systems 32*, pp. 8024–8035. Curran Associates, Inc., 2019.
- Raftery, A. E., Gneiting, T., Balabdaoui, F., and Polakowski, M. Using Bayesian Model Averaging to Calibrate Forecast Ensembles. *Mon. Weather Rev.*, 133(5):1155–1174, May 2005. ISSN 1520-0493, 0027-0644. doi: 10.1175/MWR2906.1.
- Rasp, S. and Lerch, S. Neural networks for post-processing ensemble weather forecasts. *Mon. Wea. Rev.*, 146(11):3885–3900, November 2018. ISSN 0027-0644, 1520-0493. doi: 10.1175/MWR-D-18-0187.1.
- Rasp, S., Dueben, P. D., Scher, S., Weyn, J. A., Mouatadid, S., and Thuerey, N. WeatherBench: A benchmark dataset for data-driven weather forecasting. *ArXiv200200469 Phys. Stat*, June 2020.
- Schaeybroeck, B. V. and Vannitsem, S. Ensemble post-processing using member-by-member approaches: Theoretical aspects. *Q. J. R. Meteorol. Soc.*, 141(688):807–818, 2015. ISSN 1477-870X. doi: 10.1002/qj.2397.
- Schefzik, R., Thorarinsdottir, T. L., and Gneiting, T. Uncertainty Quantification in Complex Simulation Models Using Ensemble Copula Coupling. *Stat. Sci.*, 28(4):616–640, November 2013. ISSN 0883-4237, 2168-8745. doi: 10.1214/13-STS443.
- Scheuerer, M., Switanek, M. B., Worsnop, R. P., and Hamill, T. M. Using Artificial Neural Networks for Generating Probabilistic Subseasonal Precipitation Forecasts over California. *Mon. Weather Rev.*, 148(8):3489–3506, July 2020. ISSN 1520-0493, 0027-0644. doi: 10.1175/MWR-D-20-0096.1.
- Schulz, B. and Lerch, S. Machine learning methods for post-processing ensemble forecasts of wind gusts: A systematic comparison. *ArXiv210609512 Phys. Stat*, June 2021.
- Steininger, M., Abel, D., Ziegler, K., Krause, A., Paeth, H., and Hotho, A. Deep Learning for Climate Model Output Statistics. *ArXiv201210394 Phys.*, December 2020.
- Taillardat, M., Mestre, O., Zamo, M., and Naveau, P. Calibrated Ensemble Forecasts Using Quantile Regression Forests and Ensemble Model Output Statistics. *Mon. Weather Rev.*, 144 (6):2375–2393, June 2016. ISSN 1520-0493, 0027-0644. doi: 10.1175/MWR-D-15-0260.1.
- Toth, Z. and Kalnay, E. Ensemble Forecasting at NMC: The Generation of Perturbations. *Bull. Am. Meteorol. Soc.*, 74(12): 2317–2330, December 1993. ISSN 0003-0007, 1520-0477. doi: 10.1175/1520-0477(1993)074(2317:EFANTG)2.0.CO;2.
- Vaswani, A., Shazeer, N., Parmar, N., Uszkoreit, J., Jones, L., Gomez, A. N., Kaiser, L., and Polosukhin, I. Attention Is All You Need. *ArXiv170603762 Cs*, December 2017.
- Wang, X., Girshick, R., Gupta, A., and He, K. Non-local Neural Networks. *ArXiv171107971 Cs*, April 2018.
- Xiong, R., Yang, Y., He, D., Zheng, K., Zheng, S., Xing, C., Zhang, H., Lan, Y., Wang, L., and Liu, T. On Layer Normalization in the Transformer Architecture. In *International Conference on Machine Learning*, pp. 10524–10533. PMLR, November 2020.
- Zhang, H., Dauphin, Y. N., and Ma, T. Fixup Initialization: Residual Learning Without Normalization. *ArXiv190109321 Cs Stat*, March 2019.

## A. Additional results

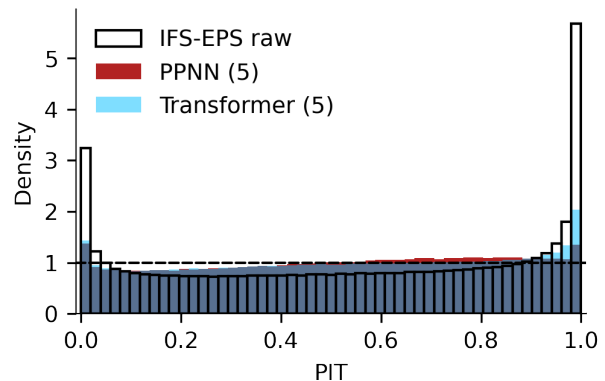


Figure 3. Probability integral transform (PIT) histogram for the IFS raw data, the PPNN (5) experiment, and the Transformer (5) experiment for all grid point and time steps within the test dataset. The PIT histogram of the IFS-raw and Transformer (5) experiment results out of a rank histogram. Because of the parametric approach, the PPNN histogram originates out of the Gaussian conditional probability functions.